

Molecular abundances in star-forming regions

Mario Tafalla¹

¹ Observatorio Astronómico Nacional (IGN)

Abstract

Star formation occurs in the densest and coldest parts of molecular clouds. In these regions, neither H₂ nor He emit appreciable radiation, and because of that, the study of the cold star-forming gas depends critically on the observation of low-abundance tracer species like CS, HCN, or NH₃. In recent years, evidence has emerged that many of these tracers suffer significant changes in abundance during the process of core contraction, and because of that, we now know that the observational appearance of many star-forming regions changes systematically as the gas becomes denser. Most of these chemical changes result from the fact that at low temperatures and high densities, molecules stick to the dust grains and cannot evaporate back into the gas phase. As a result, classical dense gas tracers like CS and HCN freeze out under the very same gas conditions that they were supposed to trace, and thus become unreliable tools to study cold, star-forming gas. Fortunately, a small number of species seem to benefit from the freeze out of CO, and they increase in abundance, at least in the range of typical densities of low-mass starless cores. Nitrogen-bearing molecules like NH₃, in particular, have become favored tracers of core material, given that their abundance increases in CO-depleted regions. Some deuterated ions, like H₂D⁺, also favor CO-depleted gas, and their abundance enhancement under these conditions is responsible for the high degree of deuterium fractionation observed in some star-forming regions. This new understanding of dense core chemistry offers a new tool to study dense core evolution, and a number of searches to identify cores at the earliest stages of contraction are in progress.

1 Introduction

Interstellar gas is the raw material of the star-formation process. It forms large clouds of thousands or even millions of solar masses, and it is mostly composed of hydrogen molecules and helium atoms. At the very low temperatures typical of the clouds (10–20 K), both H₂ and He are in their fundamental energy state and do not emit detectable radiation. Because

of that, our eyes and telescopes are blind to more than 99% of the cloud gas, and the study of star formation depends critically on the observation of minor tracers.

The first minor tracer to be identified was not a molecule, but the solid particles we call interstellar dust and contain about 1% of the cloud mass. These particles block the light from background stars and give rise to apparent stellar voids in optical plates, like those identified for the first time by E.E. Barnard more than a century ago [2]. The discovery of the CO molecule [30] provided the most widely used tracer of molecular gas, which has an abundance close to 10^{-4} with respect to H_2 . The study of the dense cores where stars form require the observation of even more rare species, like NH_3 , CS, or HCN, which have abundances of 10^{-8} – 10^{-9} . It is sobering to think that when studying in detail a given star-forming region, we are often observing one molecule in a billion and assuming that the rest of the molecules are behaving the same way.

Our reliance on low-abundance tracers makes our observations extremely sensitive to chemistry. Chemical reactions can change molecular abundances by orders of magnitude, and these changes can dominate the appearance of molecular cloud maps. Understanding the main chemical processes of the gas is therefore a first step to interpret molecular cloud observations.

Every step of the star-formation sequence is characterized by a set of chemical processes. Before the star is born, a dense core lacks internal energy sources, and the gas is cold and relatively dense. As we will see below, these conditions favor a chemistry dominated by molecular freeze out and deuterium fractionation, and those are indeed the chemical characteristics of pre-stellar cores. Once a central energy source is formed, the core gas is both heated by the radiation from the protostar and shocked by its bipolar outflow, and these energetic processes change the chemistry of the gas to one characterized by ice evaporation and high-temperature reactions. Due to practical limitations, this article will only deal with the low-energy processes characteristic of the pre-stellar phases. Recent reviews by [11] and [5] provide a more complete description of both the theory and observations of these early phases of star-formation. The reader interested in the energy dominated processes characteristic of the later phases is referred to a number of excellent recent reviews, such as the one by [27].

2 Chemical differentiation of dense cores

To study the chemical processes characteristic of the pre-stellar phases, we focus on regions with simple physical conditions. Dense cores and globules are the simplest star-forming places that we know of, and are well-studied sites of low-mass star formation. They appear in optical plates as regions of enhanced obscuration, and molecular observations reveal that they contain one or a few solar masses of gas in a centrally concentrated configuration close to gravitational equilibrium, e.g., [3].

During the 1980s and 1990s, there was growing evidence that even the simplest star-forming regions may have a rather complex chemical composition. Observations of dense gas tracers like CS and NH_3 , expected to probe similar gas conditions, often provided very

different views of the same star-forming core, with different spatial extents and positions for the emission maximum [31, 20]. Unfortunately, these early observations did not have enough angular resolution to distinguish a clear pattern in the emission distributions, and no tracer of the gas seemed at the time superior to the others in terms of chemical stability and simple excitation.

This situation changed radically at the end of the 1990s, when it was realized, somewhat paradoxically, that the most faithful tracer of the gas component is the dust, in particular when observed as an agent of extinction [12]. This result, together with the significant increase in angular resolution provided by single dishes and interferometers of the time, quickly showed a common pattern of molecular abundance in starless cores and globules: carbon-bearing species, like CO and CS, tend to disappear from the gas phase in the high density centers of the cores, while nitrogen-bearing species like NH₃ and N₂H⁺ survive almost unaffected up to much higher densities [13, 9, 6, 24]. As a result of this differentiated abundance pattern, the appearance of a core depends strongly on the tracer used to map it, and ranges from being centrally concentrated when observed in the dust continuum, NH₃, or N₂H⁺ to appearing like a more-or-less continuous ring when observed in CO and CS (or their isotopologues). This pattern is illustrated in Fig. 1 for the case of the L1517B core in Taurus-Auriga.

3 Characterizing the physical structure of starless cores

If the chemical composition of a core can dominate its appearance in the maps, it is critical to characterize the behavior of each molecule that can potentially serve as a dense gas tracer, and determine whether it is as sensitive to central depletion as CO and CS. This type of analysis requires observing the emission from a large number of species towards a series of cores that have a regular geometry, and converting the observed intensities into a pattern of abundances by modelling in detail the transfer of radiation. In [25, 26], we have presented this type of analysis for two dense starless cores in the Taurus-Auriga cloud known for their regular geometry: L1498 and L1517B.

Figure 2 presents maps of the 1.2 mm continuum dust emission from the L1498 and L1517B cores. As can be seen, both cores are centrally concentrated and close-to-round in shape, appearing therefore as good candidates for spherically symmetric modelling. In order to use the two cores as observational laboratories of dense core chemistry, we first need to characterize their physical properties, and in particular, their internal distribution of density, temperature, and non-thermal motions.

To derive the density structure of the cores, we use the 1.2 mm continuum emission and assume that it arises from a spherical distribution of dust having constant temperature and emissivity. As the dust emission is optically thin, its radial profile is proportional to the dust column density, which in turn is proportional to the gas column density if the gas-to-dust ratio is constant (which is assumed). To fit the data of a core, we therefore start by assuming a density distribution, and calculate the expected emission profile for a given choice of dust parameters (10 K temperature and emissivity of 0.005 cm² g⁻¹). This emission profile is then compared to the observed radial profile after simulating an observation. In case of a

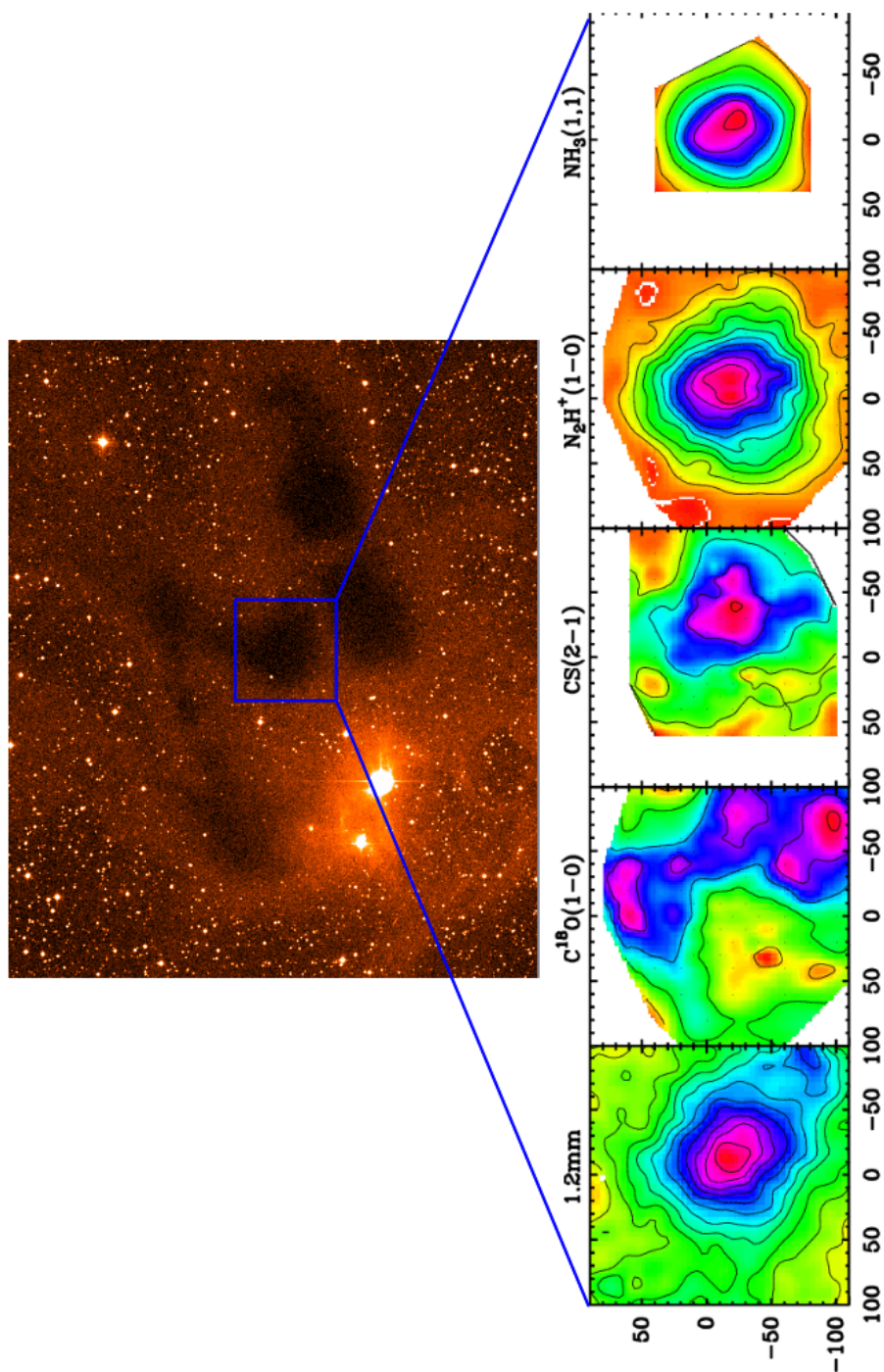


Figure 1: *Left:* optical DSS plate showing a general view of the L1517 dark cloud and its multiple cores. *Panels to the right:* dust and molecular emission maps of the L1517B core illustrating its chemically differentiated structure (from [25]).

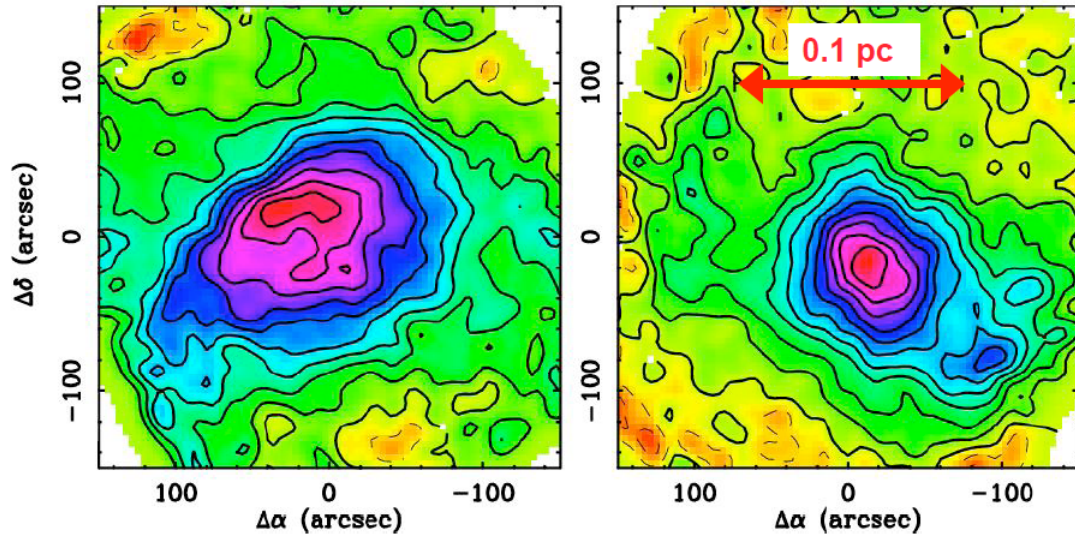


Figure 2: 1.2 mm dust continuum maps of the L1498 and L1517B starless cores illustrating their size, close-to-circular shape, and concentrated density structure.

mismatch, a new density model is assumed and the process is repeated until finding a fit. To simplify the procedure, we have modeled the cores using a simple analytic expression of the form

$$n(r) = \frac{n_0}{1 + (r/r_0)^\alpha}, \quad (1)$$

where n_0 , r_0 , and α are three free parameters that correspond to the central density, the half maximum radius, and an asymptotic power law. As the top panel in Fig. 3 shows, these density profiles provide an acceptable fit to the observed emission profile, as it combines a significant flattening towards the center and an almost power-law behavior at large radii.

To estimate the temperature profile of the gas, we use observations of $\text{NH}_3(1,1)$ and $\text{NH}_3(2,2)$. The combination of these two transitions constitutes a well-known gas thermometer under molecular cloud conditions [29], and the NH_3 molecule, being one of the few molecular species that remains in the gas phase at high densities, traces the totality of the core material (see below). As the middle panel in Fig. 3 shows, the observations of L1498 are consistent with a constant gas temperature at all radii, and a similar result is obtained for L1517B (see [25]).

The final parameter of our physical model of the cores is the non-thermal velocity component. As with the temperature, we rely on NH_3 observations to ensure that our estimate applies to even the densest parts of the cores. For that, we fit the hyperfine structure of the $\text{NH}_3(1,1)$ spectrum and determine the NH_3 linewidth corrected for optical depth effects. To this linewidth, we subtract in quadrature the thermal component at the estimated gas temperature and derive as a residual a non-thermal component, e.g., [18]. As shown in the bottom panel of Fig. 3, this non-thermal component is small, and approximately corresponds

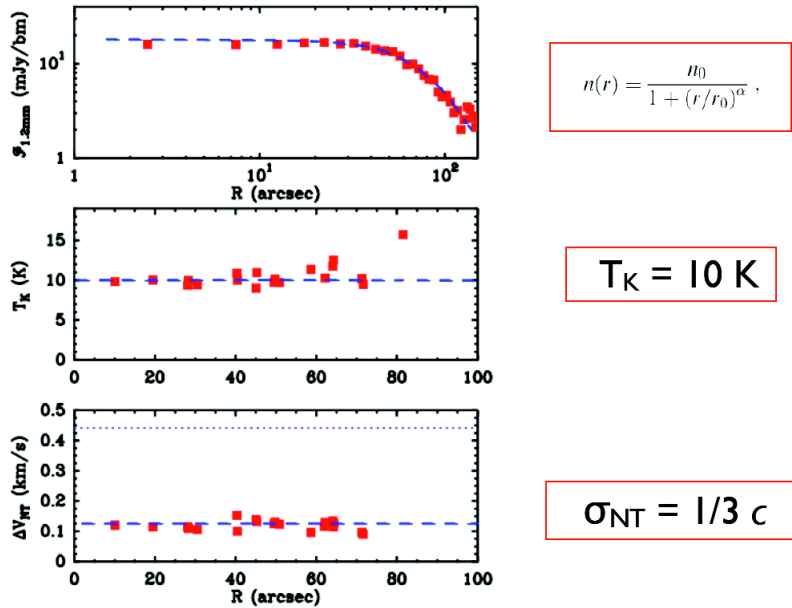


Figure 3: Physical modeling of the L1498 starless core. *Top panel:* density profile from a fit to the 1.2 mm dust continuum. *Middle:* temperature profile from the analysis of NH_3 emission. *Bottom:* non-thermal linewidth from hyperfine fits to the $\text{NH}_3(1,1)$ spectra.

to one third of the sound speed. Such low value, also obtained in L1517B, is a remainder of the quiescent state of the gas in the cores, and an indication that the non-thermal motions do not contribute appreciably to the equilibrium balance of the core: the ratio of non-thermal to thermal gas pressure is $(\sigma_{\text{NT}}/c)^2$, which is approximately 1/9 for both L1498 and L1517B.

4 Modelling the molecular emission

Once the physical structure of the cores has been determined, we can consider the cores as laboratories where the different molecular abundances can be determined from observations. We have attempted to characterize the chemical composition of L1498 and L1517B as completely as possible by making more than 20 maps of each core using transitions of 13 molecular species, and a small, representative sample of them is shown in the upper panels of Fig. 4. To derive a set of molecular abundances from these maps, we need to model the radiative transfer for each species and find an abundance profile that predicts an intensity distribution that matches the observations. As before, we model each core assuming spherical symmetry, and convert the emission in the maps into a set of radial profiles of intensity (as illustrated by the panels in the bottom half part of Fig. 4).

We have modeled the radiative transfer of each species using a modified version of the Monte Carlo code from [7], to which we have added the most recent collision rates and a simplified treatment of the hyperfine component for species like N_2H^+ and NH_3 . As a first

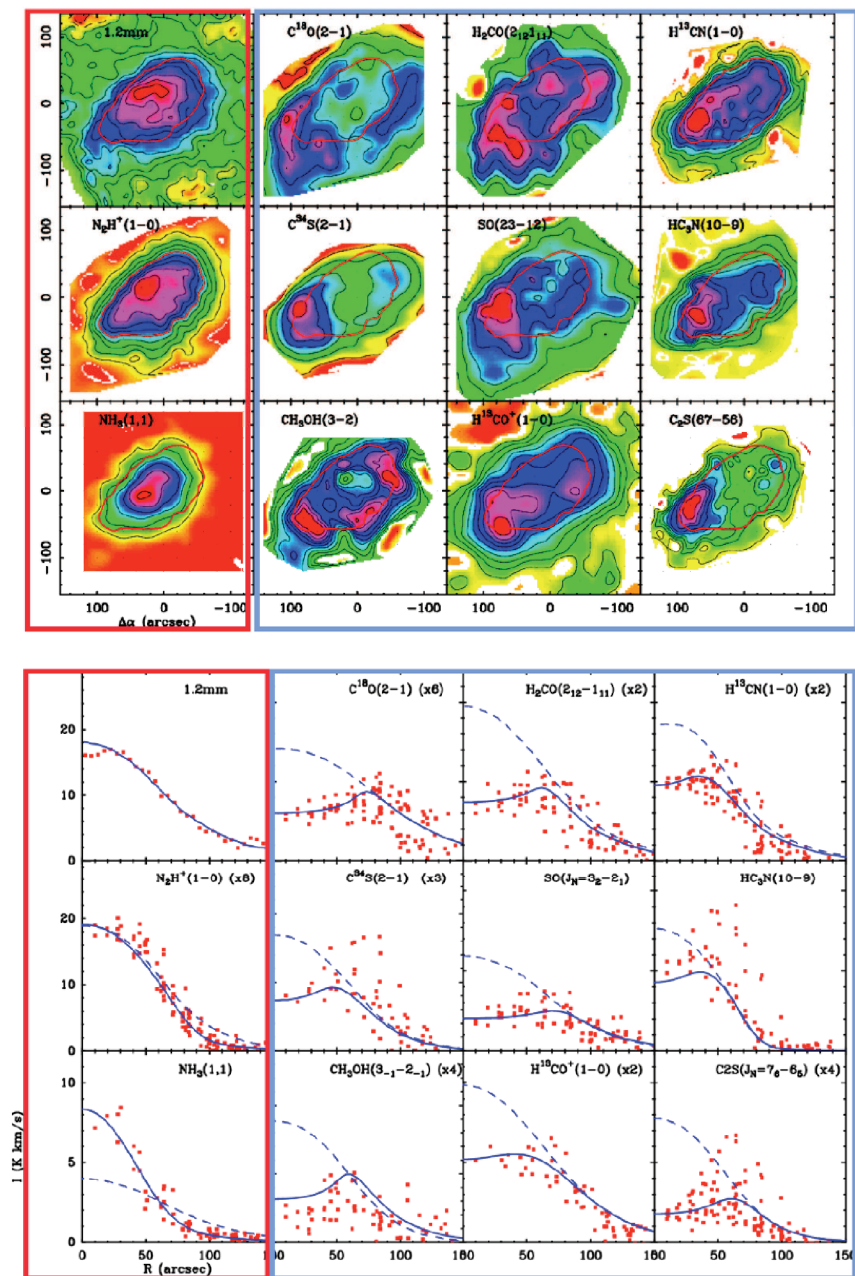


Figure 4: Chemical modeling of the L1498 starless core. *Top panels*: integrated intensity maps for a sample of observed transitions. *Bottom panels*: radial profiles of emission of the maps in the top panels together with radiative transfer models. Dashed lines indicate models with constant abundance and solid lines indicate the best fits. See text for further details.

step, we have attempted to fit the emission radial profiles assuming constant abundance for all species, and determining the value of the abundance that best fits the outer part of the core. As Fig. 4 shows, for most species, a constant abundance model (dashed lines) over-predicts the central intensity by a large factor, and is in significant disagreement with the apparent decline or flattening of the emission towards the core center shown by the data. To fit the central part of the profiles, most species require a significant drop in the abundance at high densities, and we have modeled this drop using a simple step function. With this function, the molecular abundance is kept constant for all radii larger than a given r_d , which we call the depletion radius, and inside this radius, the abundance is considered negligible (actually 10^{-4} times the outer abundance to avoid numerical problems caused by a zero abundance).

As can be seen in Fig. 4, models with a central abundance drop fit well most radial profiles, and in particular, those of C-bearing species such as CO, CS, HCO⁺ and HCN (this result is repeated in L1517B). The need for a central abundance drop is indeed a general trend in our molecular sample, and the only exceptions that we find are N₂H⁺ and NH₃. As shown in Fig. 4 the N₂H⁺(1–0) radial profile can be fitted reasonably well with an almost constant abundance model, and the same behavior is seen in L1517B. For NH₃, a constant abundance model underestimates the central intensity, and it is necessary to add a significant increase of abundance toward the core center. This increase, also found in L1517B, is unique to NH₃, and shows that this species is a sensitive tracer of the inner core gas (which justifies its use to estimate the core gas temperature and the non-thermal velocity component).

5 Origin of the observed abundance patterns

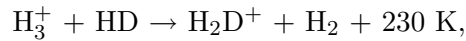
The observational discovery of chemical inhomogeneities in the interior of dense cores has been accompanied by an intense effort in chemical modeling (e.g., [4, 1]). As a result, there is a consensus that the observed abundance drops arise from the condensation or freeze out of gas-phase molecules onto the cold dust grains near the core centers. The physics of the freeze out process has been investigated for some time, and in fact, it had been somewhat of a mystery why interstellar molecules do not disappear more often from the gas phase, e.g., [15]. The reason for this expectation is that molecules collide with dust grains on timescales on the order of $t_d \sim 5 \times 10^9/n(\text{H}_2)$ yr. For typical core densities of few 10^4 cm^{-3} , the t_d timescale is on the order of 10^5 yr, which is at least 10 times shorter than the expected dense core lifetimes, e.g., [14]. As the sticking probability for these collision is close to unity [8] and thermal evaporation from the dust surface is not efficient at temperatures of about 10 K [15], unless there is an efficient non-thermal mechanism for releasing the molecules back to the gas phase, significant molecular freeze out is expected to occur in a t_d timescale.

If the abundance drop observed for the carbon-bearing molecules can be understood as resulting from molecular freeze out, explaining the behavior of nitrogen-bearing species requires additional considerations. In the case of N₂H⁺, for example, it is thought that the survival of this molecule in the gas phase is a direct consequence of CO freeze out. According to chemical models, N₂H⁺ is constantly generated in the gas phase by the reaction of N₂ with H₃⁺, a process that is balanced by the destruction of N₂H⁺ with CO [1]. As CO is 7 orders of magnitude more abundant than N₂H⁺, CO freeze out, even if partial, has profound

consequences for the N_2H^+ chemistry: it decreases the abundance of its main destroyer. As a result, even if N_2 (N_2H^+ parent) also suffers freeze out in the core interior, the significant decrease of CO dominates the N_2H^+ chemistry, with the consequence that N_2H^+ remains significantly abundant in the gas phase at typical core densities (N_2H^+ seems to freeze out at higher densities, where the disappearance of CO cannot compensate the effect, see [19]).

6 Further consequences of freeze out

N_2H^+ is not the only gas-phase species enhanced as a result of CO freeze out. The abundance of deuterated species is also sensitive to the amount of CO in the gas phase, and significant deuterium fractionation is expected to occur under conditions of CO depletion. This is so because deuteration at low temperatures occurs via the slightly exothermic reaction



which under dense core conditions enhances selectively the abundance of H_2D^+ over the cosmic D/H ratio [17]. Ion-molecule reactions can later pass down the deuterium atom to different molecular species, in particular to CO and form the deuterated variety DCO^+ . Under conditions of CO freeze out, H_2D^+ is expected to be enhanced (as its main destroyer is depleted), and this allows to pass down the D atom to other species like N_2H^+ , to form N_2D^+ . A high abundance of H_2D^+ even allows further reactions with D to produce the doubly and triply deuterated forms D_2H^+ and D_3^+ , which in turn can pass the double and triple deuterium group to other species like NH_3 and CH_3OH , forming doubly and triply deuterated varieties. Over the last few years, this deuteration scheme has been beautifully confirmed, first by the detection of enhanced H_2D^+ abundance in dense cores [10], and later by the detection of D_2H^+ [28]. Also, double and triple deuterated varieties of species like NH_3 have been recently detected [22, 16], providing a significant level of self consistency to our picture of the chemical conditions under CO freeze out.

Another expectation under CO freeze out conditions is that the amount of CO ice on grains will increase significantly towards cold and dense regions. The amount of CO ice on grains can only be measured along lines of sight having bright IR sources, so no detailed maps of solid CO are yet possible for dense cores. [21] has measured the intensity of the CO stretch band at $4.67 \mu\text{m}$ towards a sample of IR sources behind the Oph-F core and found that, indeed, the relative abundance of CO ice with respect to H_2O ice increases towards the densest parts of the core. This result is again in good agreement with the expectation from chemical models, and shows that a significant fraction of CO molecules make the transition from gas to solid as the density of the gas increases.

7 Using core composition to track core evolution

Molecular freeze out provides a promising tool to time the evolution of dense cores. As shown before, the time scale of freeze out is simply given by the frequency of collisions between gas

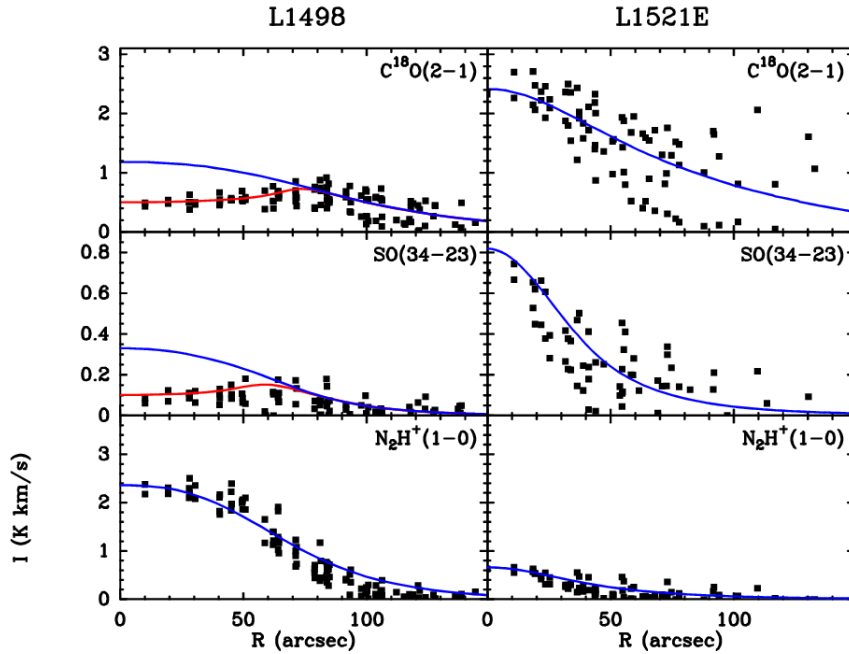


Figure 5: Comparison between emission radial profiles from L1498 and L1521E. Blue lines represent constant abundance models and red lines represent models with central depletion.

molecules and dust grains. Thus, if we can estimate the degree of freeze out occurring in a given core, we may be able to reconstruct the history of core contraction.

CO freeze out, in addition, makes a core change its composition and appearance to observations as it ages, and this effect provides a simple way to distinguish relatively evolved cores (but still starless) from more-recently condensed systems. Key to this distinction is the observation of a core in molecular species with different sensitivity to freeze out, such as CO and N_2H^+ : young cores are expected to present low CO freeze out and low N_2H^+ abundance, while evolved cores should be characterized by strong CO freeze out and high N_2H^+ abundance.

Using CO and N_2H^+ as indicators of core evolution, [23] identified the L1521E condensation in Taurus as an unusually chemically-young starless core. This core has a number of signatures of not having yet suffered CO freeze out, or having suffered it minimally. These signatures are illustrated in Fig. 5 with a comparison between L1521E and the evolved (but still starless) L1498 core we have studied before. As shown in the figure, while L1498 presents strong evidence for central depletion of C^{18}O and SO, the emission from L1521E can be fitted with a model having constant C^{18}O and SO abundances. At the same time, the abundance of N_2H^+ in L1521E is 8.5 times lower than in L1498, which is consistent with the idea that there is more N_2H^+ -destroying CO at the center of L1521E than in L1498.

Although the chemical composition of L1521E clearly differs from that of more evolved cores, its physical structure is comparable to that of L1498 and L1517B. The density profile of L1521E, for example, peaks around $3 \times 10^5 \text{ cm}^{-3}$, while those of L1498 and L1517B peak

in the range $1\text{--}2 \times 10^5 \text{ cm}^{-3}$. Also, the degree of central concentration of L1521E is similar to that of L1517B. How a chemically young core like L1521E has developed the density structure of an evolved core is still a mystery. Rapid contraction is a possibility, e.g., [1], but the subsonic linewidths observed towards L1521E set a very stringent limit to the maximum contraction speed allowed for the gas.

To better understand the properties of young condensations and to clarify the status of L1521E, it seems necessary to expand the sample of cores with evidence for chemical youth. To do so, we have started a systematic study of a sample of 12 cores that have evidence for very different NH_3 intensities from previous observations, e.g., [3], and that are likely to span a range of NH_3 abundances and therefore evolutionary stages. This work combines dust continuum observations with line mapping in N_2H^+ and NH_3 , and shows that although rare (or hard to identify), a number of chemically young cores are present in the Taurus-Auriga complex. What seems unique in L1521E is its extreme density profiles: all other chemically young cores in our sample are less dense and often less centrally concentrated than L1521E, and this suggests that L1521E has suffered a more extreme form of contraction than most other cores in the cloud. Although still preliminary, this analysis shows how our new understanding of core chemical composition makes it finally possible to reconstruct the history of dense core contraction, and therefore to explore the earliest possible stages of the star-formation sequence (Canay & Tafalla, in preparation).

References

- [1] Aikawa, Y., Herbst, E., Roberts, H., & Caselli, P. 2005, *ApJ*, 620, 330
- [2] Barnard, E.E. 1907, *ApJ*, 25, 218
- [3] Benson, P.J., & Myers, P.C. 1989, *ApJSS*, 71, 89
- [4] Bergin, E.A., & Langer W.D. 1997, *ApJ*, 486, 316
- [5] Bergin, E.A., & Tafalla, M. 2007, *ARAA*, 45, 339
- [6] Bergin, E.A., Alves, J., Huard, T., & Lada, C.J. 2002, *ApJ*, 570, L101
- [7] Bernes, C. 1979, *A&A*, 73, 67
- [8] Bisschop, S.E., Fraser, H.J., Öberg, K.I., van Dishoeck, E.F., & Schlemmer, S. 2006, *A&A*, 449, 1297
- [9] Caselli, P., Walmsley, C.M., Tafalla, M., Dore, L., & Myers, P.C. 1999, *ApJ*, 523, L165
- [10] Caselli, P., van derTak, F.F.S., Ceccarelli, C., & Bacmann, A. 2003, *A&A*, 403, L37
- [11] Di Francesco, J., Evans, N.J., II, Caselli, P., et al. 2007, in *Protostars and Planets V*, Reipurth et al. eds., Tucson, AZ: Univ. Ariz. Press, 17
- [12] Kramer, C., Alves, J., Lada, C.J., et al. 1999, *A&A*, 342, 257
- [13] Kuiper, T.B.H., Langer, W.D., & Velusamy, T. 1996, *ApJ*, 468, 761

- [14] Lee, C.W., & Myers, P.C. 1999, *ApJSS*, 123, 233
- [15] Leger, A., Jura, M., & Omont, A. 1985, *A&A*, 144, 147
- [16] Lis, D.C., Roueff, E., Gerin, M., et al. 2002, *ApJ*, 571, L55
- [17] Millar, T.J., Bennett, A., & Herbst, E. 1989, *ApJ*, 340, 906
- [18] Myers, P.C. 1983, *ApJ*, 270, 105
- [19] Pagani, L., Pardo, J.R., Apponi, A.J., et al. 2005, *A&A*, 429, 181
- [20] Pastor, J., Buj, J., Estalella, R., Lopez, R., Anglada, G., & Planesas, P. 1991, *A&A*, 252, 320
- [21] Pontoppidan, K.M. 2006, *A&A*, 453, L47
- [22] Roueff, E., Tiné, S., Coudert, L.H., Pineau des Forêts, G., Falgarone, E., & Gerin, M. 2000, *A&A*, 354, L63
- [23] Tafalla, M., & Santiago, J. 2004, *A&A*, 414, L53
- [24] Tafalla, M., Myers, P.C., Caselli, P., Walmsley, C.M., & Comito, C. 2002, *ApJ*, 569, 815
- [25] Tafalla, M., Myers, P.C., Caselli, P., & Walmsley, C.M. 2004, *A&A*, 416, 191
- [26] Tafalla, M., Santiago, J., Myers, P.C., Caselli, P., Walmsley, C.M., & Crapsi, A. 2006, *A&A*, 455, 577
- [27] van Dishoeck, E.F., & Blake, G.A. 1998, *ARAA*, 36, 317
- [28] Vastel, C., Phillips, T.G., & Yoshida, H. 2004, *ApJ*, 606, L127
- [29] Walmsley, C.M., & Ungerechts, H. 1983, *A&A*, 122, 164
- [30] Wilson, R.W., Jefferts, K.B., & Penzias, A.A. 1970, *ApJ*, 161, L43
- [31] Zhou, S., Wu, Y., Evans, N.J., II, Fuller, G.A., & Myers, P.C. 1989, *ApJ*, 346, 168